1 2 3

A&A manuscript no.
(will be inserted by hand later)

Your thesaurus codes are:
06(08.14.2; 08.09.2 RX J1940.1−1025; 08.13.1; 13.25.5)

ASTRONOMY
AND
ASTROPHYSICS
20.6.1995

RX J1940.1−1025 — A new asynchronous AM Her system

S. Friedrich[1,*], R. Staubert[1,*], G. Lamer[1], M. König[1], R. Geckeler[1], M. Bässgen[1,**], W. Kollatschny[2,*], R. Östreicher[3,*], S. D. James[4,***], and R. K. Sood[4,***]**

[1] Institut für Astronomie und Astrophysik, Astronomie, Universität Tübingen, Waldhäuserstr. 64, D-72076 Tübingen, Germany
[2] Universitäts-Sternwarte Göttingen, Geismarlandstr. 11, 37083 Göttingen, Germany
[3] Landessternwarte, Königstuhl, 69117 Heidelberg, Germany
[4] University of New South Wales, ADFA, Canberra, Australia

Received date; accepted date

Abstract. We present optical spectroscopy and white light photometry of RX J1940.1−1025 over a period of one year. From the photometry two periods can clearly be distinguished. The shorter one with 12116.3s is also the period of the radial velocities of the narrow emission line components and the period of narrow dips also seen in the X-ray data. This shorter period is interpreted as the orbital period. The longer period of 12151s is also present in the X-ray data and is interpreted as the spin period of the white dwarf. We find a phase modulation of the X-ray lightcurve with the beat period of 49.5 days.

Our measurement of circular polarization of about 2% confirms the conjecture that RX J1940.1−1025 is an AM Her system.

Key words: cataclysmic variables – stars: individual: RX J1940.1−1025 – stars: magnetic fields – X-rays: stars

1. Introduction

The Seyfert Galaxy NGC 6814 was long believed to emit periodically modulated X-ray flux with a period of about 3.4 hours (Mittaz et al. 1989). From ROSAT observations during April 1993 Madejski et al. (1993) were able to conclude that another X-ray source in the field of view, about 37 arc min to the west of NGC 6814, was emitting periodically modulated flux with a period of (12142 ± 20)s. This object was identified with an optical counterpart showing an emission line spectrum similar to that of a cataclysmic variable (Rosen et al. 1993). These findings were confirmed by Staubert et al. (1994) (hereafter Paper I).

Cataclysmic variables are binary systems with a white dwarf primary and a red dwarf secondary. The secondary fills its Roche lobe and matter flows via the Lagrangian point on to the white dwarf. Due to momentum conservation matter cannot fall directly on to the primary, but forms an accretion disk. This scenario is typical for the majority of "normal" or nonmagnetic cataclysmic variables (hereafter CVs). In the case of a magnetic primary one can distinguish two classes: the DQ Herculis and the AM Herculis systems. The characteristic differences between these two classes are the asynchronous rotation of the primary, the low polarization and absence of Zeeman absorption features in DQ Her versus the synchronous rotation and high polarization in AM Her systems. DQ Her systems may form a (disturbed) accretion disk, whereas in AM Her systems no accretion disk is formed because of the existence of a strong magnetic field.

Up to recently only two asynchronously rotating AM Her systems were known: BY Cam and V1500 Cyg. In both systems the orbital period is longer than the spin period. For V1500 Cyg, which is Nova Cygni 1975, this can be explained by the interaction of the binary with the envelope and the wind of the white dwarf, after the nova explosion (Stockman et al. 1988). RX J1940.1−1025 is the third asynchronously rotating AM Her system.

In Paper I we confirmed the observations of Madejski et al. (1993) and presented radial velocity data for Hα, from which we concluded the existence of a second period of (12120 ± 3)s, in addition to the (12143 ± 9)s period seen in X-ray data. In this paper we present new spectral data, white light photometry, and additional X-ray data. Our new data support the conclusions of Paper I. As we already concluded from early photometric measurements (Friedrich et al. 1994), both the X-ray period and the radial velocity period can be discerned in the optical light curve. In Sections 2 to 5 we present our observations,

Send offprint requests to: S. Friedrich

* Visiting Astronomer, German-Spanish Astronomical Center, Calar Alto, operated by the Max-Planck-Institut Heidelberg jointly with the Spanish National Commission for Astronomy

** Visiting Astronomer, European Southern Observatory, La Silla, Chile

*** Visiting Astronomer, Mount Stromlo and Siding Spring Observatories, Australia while in Section 6 we develop a scenario which does explain the observations (see also Staubert et al. 1995).

2. X-Ray Observations

During April and October 1992 and April 1993 pointed ROSAT observations of NGC 6814 were performed by Staubert et al. (Paper I) and Madejski et al. (1993), respectively. RX J1940.1−1025 was in the field of view in each observation, but more or less behind a support strut of the Position Sensitive Proportional counter (PSPC). Therefore in October 1993 a further ROSAT observation pointed on RX J1940.1−1025 was performed by Staubert.

The April 1992 observation was mostly not usable for spectral and timing analysis, as RX J1940.1−1025 was exactly obstructed by the strut. Light curves of the October 1992 data were corrected for the influence of the strut in such a way, that the light curves could be directly compared to the light curves of the October 1993 observation, which were not hampered by a strut. Spectral fits are not influenced by the strut, and therefore no corrections were made.

2.1. Time Series Analysis

Due to the low-earth orbit of the ROSAT-satellite all light curves have unavoidable gaps. In searching for periodicities, two sets of techniques are generally used: those based on the Discrete Fourier Transform (Deeming 1975, Scargle 1982), and those based on the folding of data modulo a trial period.

In the case of the analysis of the X-ray observations of RX J1940.1−1025 we used the second type of period search technique.

From the resulting χ^2-distribution, not only the peak corresponding to the main period P_0, but also other harmonics (e.g. $P_0/3$, $P_0 - P_0/3$) were used to estimate the period. Furthermore, EXOSAT and GINGA data were reanalysed and the period determined with this technique. Although the light curves were affected by the variable, non-deterministic X-ray source NGC 6814, it was possible to improve the period estimation significantly. All the results are listed in Table 1. The weighted mean of all X-ray periods determined is (12144 ± 10)s. The period seems to be stable over at least eight years.

Table 1. Estimated periods of RX J1940.1−1025

Satellite	Observation [year/day]	Period [s]
EXOSAT	1985/289	12142±29
Ginga	1989/119	12143±13
ROSAT	1992/285	12144±22
ROSAT	1993/121	12149±32
ROSAT	1993/279	12146±34
weighted mean:		12144±10

The determination of the X-ray period can be drastically improved by combining the data of the three ROSAT observations. This has been done in various ways. First, the three possible combinations of two of the data sets were taken and χ^2 period searches performed (over the range 12100s to 12200s). This leads to distributions with regular peaks separated by $P^2/\Delta T$s from each other (ΔT is the time between two data sets, here of order 0.5 and 1 year, respectively, and P is the period itself). Second, a χ^2 distribution was produced using all three data sets simultaneously. The true period should show up as a peak in all of these distributions. This is indeed the case with a period of about 12150s to 12151s. This result was confirmed by a somewhat different method of analysis: folded profiles (with period 12150.5s) were generated for each of the three data sets. The X-ray profiles show clear "eclipse like" structures, the center of which can be used as time reference. A phase connection between the three observations was then attempted by placing integer numbers of periods between the reference times. This again leads to periods ranging between 12150s and 12151.5s. From the combined result of the various analyses described above we state for the X-ray period a most likely mean value of (12150.7 ± 0.5)s. However, the phase connection is not perfect for a constant value of P. This is not due to statistical uncertainties, but has a systematic origin. It could mean that there is a non-zero period derivative. However, we prefer the interpretation that the X-ray emitting hot spot moves with respect to the surface of the white dwarf, which is expected because the system is not synchronized (see discussion below). A linear fit through the broad X-ray eclipse timings from the three observations results in the following ephemeris:
$T_{xecl} = HJD24459540.177(2) + 0.140634(1) \cdot N'$

Folding the X-ray data with a period of 12116.3s, a narrow dip, in which the X-ray flux drops to zero, can be detected (Watson et al. 1994). We were able to derive four separate dip timings from ROSAT X-ray data from April 92, October 92, April 93 and October 93. A linear fit results in a period of 12116.32 ± 0.03s in very good agreement with the dip period from Watson et al. and the period of the corresponding optical dips. The ephemeris for the narrow X-ray dips is:
$T_{xdip} = HJD24459199.6922(7) + 0.1402352(4) \cdot N$

2.2. X-ray Spectra and Light Curves

As already outlined in Paper I the best fit model to the X-ray spectrum is a power law plus a black body component modified by interstellar absorption. The October 1993 observation results in the following values: photon index $\Gamma = 0.8 \pm 0.45$, black body temperature kT_{BB} = (76 ± 14)eV, interstellar absorption $N_H = (5.8 \pm 2.3) \cdot 10^{20}\mathrm{cm}^{-2}$. This is consistent with the October 1992 observation within 1σ errors. A relativly good fit can also be achieved for a combined black body and thermal bremsstrahlung model with a thermal bremsstrahlung temperature of kT_{TB} fixed to 20 keV and a black body temperature of (60 ± 35)eV.

Folding the X-ray light curves with a period of 12150.7s a double peak structure appears (see also Paper I). In the soft X-

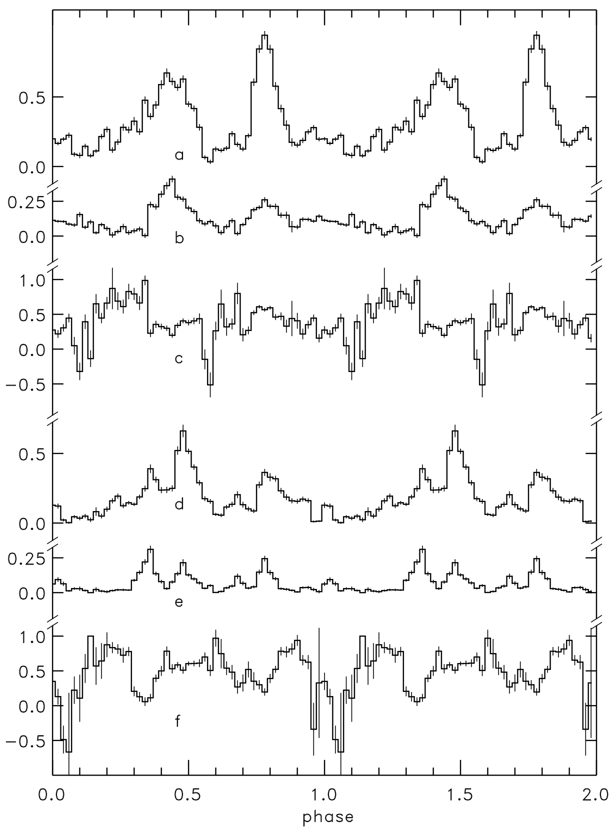

Fig. 1. Light curves (in cts/sec) and hardness ratios (HR=(H-S)/(H+S), with H and S being the observed countrates in the energy ranges $0.4 - 2.4$ keV and $0.1 - 0.4$ keV, respectively) folded with the X-ray period of 12150.7s for the October 1992 (a-c) and October 1993 (d-f) ROSAT observations: a) H light curve, b) S light curve, c) hardness ratio, d) H light curve, e) S light curve, f) hardness ratio.

ray light curves the two peaks are seperated by a 2200s (FWHM) wide gap, where the flux is low or non detectable. It is clearly seen (Fig. 1), that in October 1992 the preceeding peak is the harder one, and in October 1993 it is the softer one. Furthermore, the onset of the hard X-ray flux occurs earlier and more gradually compared to the soft band, as it is expected from a post shock region extending above the white dwarf photosphere (Cropper 1990). Additionally to the hard and soft pulse profiles for the October 1992 and 1993 observations, we show in Fig. 1 the corresponding hardness ratios. Over the most part of the period the hardness ratio is positive, and within the error never converges to the typical values for AM Her systems of between -0.57 and -0.95 given by Beuermann & Schwope (1993) for a ROSAT selected sample.

3. Optical Spectroscopy

3.1. Observations

In Table 1 of Paper I we presented details on our spectroscopic observations up to that time. Meanwhile, a further observation at the Calar Alto Observatory, Spain, was performed.

In May 1994 circular polarization spectra were taken at the Cassegrain focus of the 3.5m telescope with the "Twin"-spectrograph and an additionally implemented triple diaphragm and a quarter wave plate, which was sealed with a Savart-plate. In this telescope configuration three double spectra are produced, one double spectrum for the object and two for the sky background. The circular polarization is then calculated by the difference between the corresponding single spectra divided by their sum. We achieved simultanous coverage in two spectral regions 3500-5250 Å and 5600-7450 Å and a resolution of about 3 Å, measured by the FWHM of comparison lines in both spectral ranges. To check for intrinsic polarization of the optics, various SAO-stars and one flux standard were observed and the spectra corrected for this. All spectra were badly affected by non-reproducible interference fringes on the CCDs in both spectral regions. Therefore fine structures in the polarization spectra are not reliable.

A heliocentric correction was applied to all observing times and radial velocities.

3.2. Circular Spectropolarimetry

Since the observation in May 1994 was hampered by bad weather, only four spectra in each of the two spectral regions could be taken. Polarization could not be detected in any of the "blue" spectra, while a mean polarization of about +2% could be detected in one of the "red" spectra (Fig. 2). A strong depolarization feature is seen at the position of Hα. This is caused by the Hα emission line, which is unpolarized. There is no evidence for Zeeman absorption features in any of the spectra.

3.3. Line Profiles

The September 1993 observation is the only observation, which contiguously covers the whole period. Despite the medium resolution (about 4-6 Å) the variations of the line profiles of the Balmer lines and HeII with phase are clearly seen. In most spectra at least two different line components can be distinguished, a narrow and a broad component. The line profiles of the individual components are well represented by a sum of up to three Gaussian profiles (Fig. 3).

At no time do the line profiles show a double peaked structure, which we would expect for an accretion disk. This fact, in addition to the measured circular polarization, points to an AM Her system.

Line center and FWHM for each line component could be determined by fitting multiple Gaussian components to the line profiles. On average the narrow component of the Balmer lines and HeII shows a FWHM of 10 to 20 Å and the broad component a FWHM of about 20 to 50 Å. The FWHM of

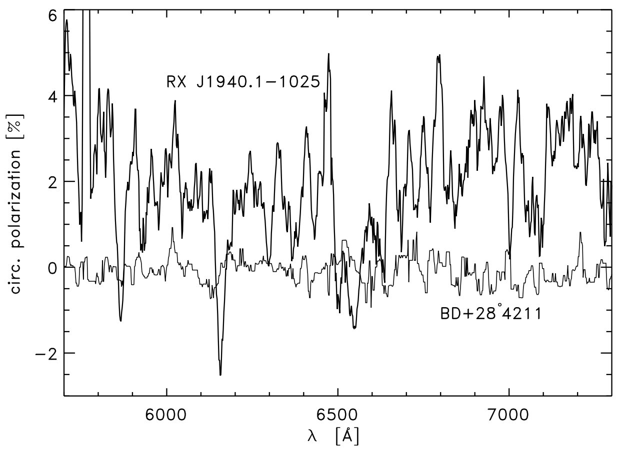

Fig. 2. Circular polarization spectrum of RX J1940.1−1025. For comparison the spectrum of the flux standard BD+28°4211, which shows no polarization, is also plotted. Clearly seen are the ripples, caused by interference fringes on the CCD.

the narrow component is significantly larger than the 2-3 Å measured for the narrow component in other AM Her systems (Cropper 1990).

3.4. Radial Velocities

The centers of the Gaussian profiles from the multiple Gaussian fit were taken as the position of the individual line components. We find the same systematic shift of the narrow line component position for all Balmer lines and the HeII line, defining a sinusoidal radial velocity curve with a mean period of (12116.0 ± 1)s for the Balmer lines and (12114.2 ± 1)s for the HeII line. In Fig. 4 we show the best fit for the radial velocity curve of the narrow component of H(alpha). While the narrow component is always identifiable, a distinction between the two broad components which are often present is not unique. Further work on this is in progress.

The short period of 12116s is consistent with the period of (12120 ± 3)s derived from radial velocity measurements of Hα alone, presented in Paper I. The former radial velocities were determined by a single gaussian fit and were therefore influenced by the broad component.

The half amplitude of the narrow component amounts to 120-130 km/s for Hα and Hβ, 160 km/s for Hγ, and 100 km/s for HeII. The offset of the radial velocities seems to increase with increasing excitation energy, which is expected for an accretion stream lifted out of the orbital plane.

4. White Light Photometry

White light photometry was performed in Tübingen with the 30cm refractor and the 40cm reflector and an ST6 CCD camera on altogether 18 nights in December 1993 and during the period May to December 1994. The camera consists of a thermoelectrically cooled TC 241 chip with 375 × 242 pixels and a 16 bit AD converter. To acquire sufficient signal to noise ratios integration times of 60 seconds for the larger and 120 seconds for the smaller instrument were chosen. Standard image processing techniques such as dark and bias subtraction and flat fielding, using a mean twilight flat, were applied to the frames. Relative photometry was done using aperture photometry techniques.

In the broad spectral response band of the CCD the amplitude of RXJ1940.1-1025 is approximately $2\overset{m}{.}6$. The accuracy of the photometry was determined both experimentally, using a set of sources on the frames with no apparent intrinsic variability (Howell et al. 1988), and theoretically, using models for signal to noise ratios of processed CCD frames (Newberry 1991). The results of both approaches show, that our relative photometry achieves accuracies better than $0\overset{m}{.}05$ down to $16\overset{m}{.}5$, depending on sky conditions.

Barycentric corrections were applied to all observation times.

Fig. 3. Line profiles of the Hα line for two different phase points. The dashed lines are the single Gaussian components.

4.1. Time Series Analysis

We applied a χ^2 period search to our entire photometric data. Significant peaks in the χ^2-distribution are detected at 12116s

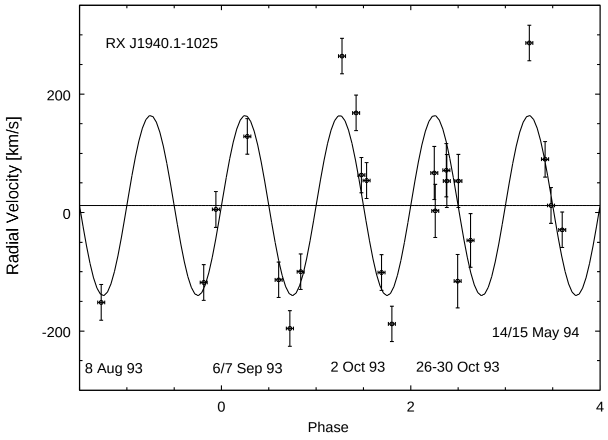

Fig. 4. Radial velocity curves for the narrow line component of Hα .

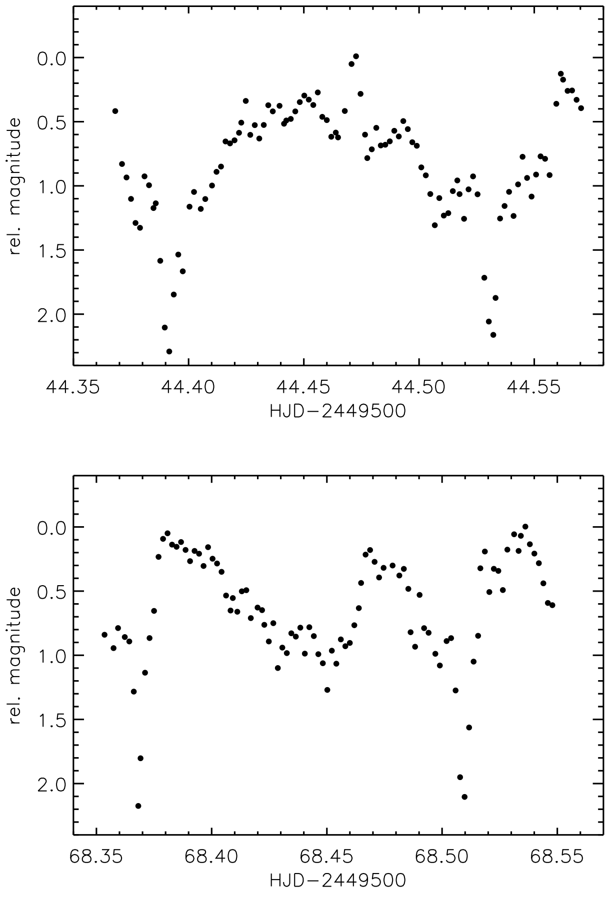

Fig. 5. Light curves of RX J1940.1−1025 taken on July 10/11 (top) and August 3/4 (bottom) .

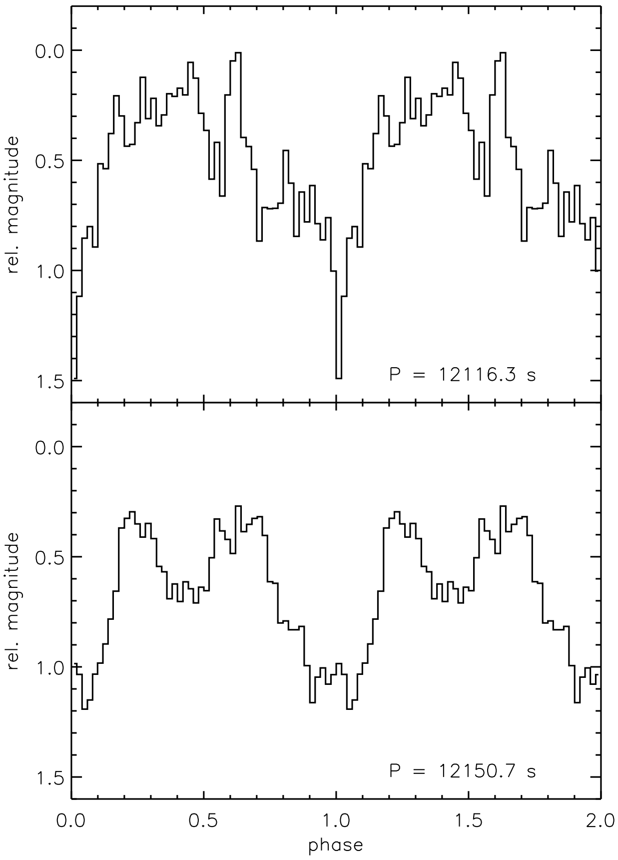

Fig. 6. Folded light curves of RX J1940.1−1025 for the two periods P=12116.3s and P=12150.7s from all photometric data. The data points belonging to the sharp dips occuring every 12116.3s have been omitted in the calculation of the lower light curve. Zero phases refer to the ephemerides given in section 4.2.

and 12150s. The shorter period is due to a narrow dip feature with $\sim 2^m$ depth and was determined by Watson et al. 1994 to (12116.2 $\pm$ 0.4)s. Modulo peaks of this period also contaminate the χ^2-distribution around 12150s. In order to exclude contamination all data points belonging to the dip feature were omitted in a second run of the period search. The χ^2-test on the modified data set yields the value (12151.3 $\pm$ 2.5) for the longer period.

Furthermore, it is possible to improve the period estimate of the short period significantly by using only the sharp dip structures in the light curves. The best fit value for the period is then (12116.24 $\pm$ 0.12)s. Combining our data with the ephemerides of the dip feature given by Watson et al. 1994 and Patterson 1994 we obtained the most accurate value of (12116.26$\pm$0.01)s. Both periods are in good agreement with the respective X-ray periods discussed in section 2.1. We therefore adopt the more accurate X-ray period (12150.7 $\pm$ 0.5)s and the mean of the X-ray and optical dip periods (12116.3 $\pm$ 0.05)s as the periods of the system.

4.2. Light Curves

In July and August 1994 more than one period could be covered during one night. Figure 5 shows two light curves from July 10/11 and from August 3/4. The narrow dips lasting about 20 minutes are conspicuous in both light curves. Whereas in the July observation the dips coincide with the minima of the broader (P=12150.7s) modulation, the dips cut into the maxima during the August observation. The phase shift by half a period is due to the separation of the two observations by 24 days, which is just half the beat period of 49.5 days.

In Fig. 6 we show folded light curves for the periods 12116.3s and 12150.7s. It is clearly seen, that the shorter period belongs to the dip, whereas the longer period fits the "remaining" light curve. The period of 12116.3s is interpreted by us as the orbital period, because it is consistent with the period of the radial velocity curves of the narrow emission line components. The longer period is interpreted as the spin period of the white dwarf, because it is dominating the X-ray light curve, and within the model framework for CVs, the X-ray radiation emerges from near the magnetic pole of the white dwarf.

From a total of nine observed dips in our photometric data, we could derive an ephemeris (HJD) for the dip:
$T_{\rm odip} = 2449568.510(1) + 0.140234(1) \cdot N$
For the deepest minimum (see Fig . 6) of the remaining light curve we got the following ephemeris (HJD):
$T_{\rm omin} = 2449540.179(1) + 0.140633(6) \cdot N'$

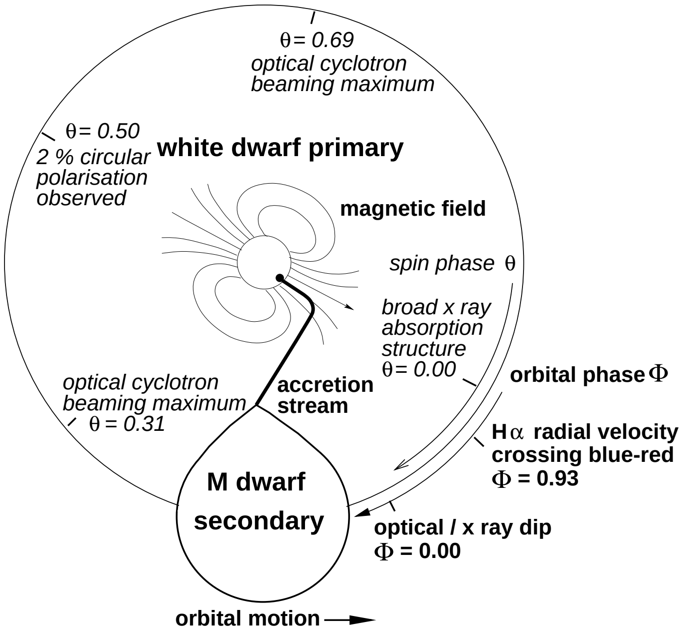

Fig. 7. Phase diagram of events around one orbit. In this time interval the changing geometry due to asynchronous rotation can be neglected. Phase zero of the orbital period ($\Phi = 0$) refers to the optical dip, while phase zero fo the spin peroid ($\Theta = 0$) refers to the broad X-ray absorption structure. The three nondetections of circular polarization were omitted; they lie between $\Theta = 0.17$ and $\Theta = 0.38$

5. Radio Observations

RX J1940.1−1025 was observed at Molonglo in July 1994 at 843 MHz. The source was not detected ($S < 0.5$mJy), consistent with the non-detection at 8.4 GHz reported by Beasley et al. (1994).

6. Results and Discussion

Looking at the photometric data we can distinguish two periods. We interpret the shorter one as the orbital period, the longer one as the spin period of the white dwarf. Taking the measured circular polarization into account, we conclude, that RX J1940.1−1025 is an AM Her system, the third out of 52 AM Her systems and AM Her candidates (Beuermann & Burwitz 1995) to be asynchronous. In contrast to BY Cam and V1500 Cyg – the other asynchronous AM Her systems – the spin period is longer than the orbital period. All three objects have very similar orbital periods. The difference between the orbital and spin period in RX J1940.1−1025 amounts to 34.4s (0.3%), the smallest of the three systems.

As already outlined by Watson et al. (1994), one can find a dip in the X-ray data with a period of 12116.3s, which is in phase with the optical dip. The optical and the X-ray dips are both about 850 seconds wide (200s ingress/egress, 450s "totality"). Therefore it is likely that one source is emitting both in the X-rays and the optical.

Furthermore, Watson et al. (1994) noted, that the ingress/egress times are too long for an eclipse by the secondary. We have calculated the eclipse properties using the Patterson (1984) relations for the secondary and the mass-radius relation for white dwarfs from Webbink (1975), treating the white dwarf primary mass as a free parameter, and compared them with the high speed photometry of Watson et al. The theoretical ingress/egress times of the photometrical dips, as expected from the duration of the totality, are too short compared with the observed ones. This holds true for all white dwarf masses above 0.2 solar masses, even if grazing eclipses of the whole white dwarf photosphere are considered. Thus the optical dips are most likely caused by absorption due to parts of the intervening accretion stream.

The radial velocity curves support this conclusion. If the dip was caused by the secondary, it would have had to be at inferior conjunction at the time of the dip. The radial velocity of the narrow line component would then be zero, if it was emitted by the illuminated surface of the secondary. In our data the dip occurs about 0.15 phase prior to maximum redshift and about 0.1 phase after the crossing from blue- to red-shifted motion. On the other hand, this contradicts the fact that the dip should occur prior to the crossing from blue- to red-shifted motion, if it is due to the accretion stream.

This behaviour can be explained if the narrow line component is not emitted from the surface of the secondary but from material in the accretion stream near the Lagrangian point (Fig. 7). An occultation by the accretion stream will then occur before maximum redshift and after the crossing of the narrow component from blue- to red-shifted motion. Since the gas emitting the narrow component is not yet influenced by the magnetic field, it follows the orbital motion. The narrow line component, which is broader than narrow line components usually observed in other AM Her spectra, and the fact that during the dip the emission lines are still detectable (Watson et al. 1994), speak in favour of this idea.

The absence of an eclipse by the secondary constrains the inclination of the system to be lower than 69° (73°) for an 0.5 (1.0) solar mass white dwarf primary. Additionally, the presence of absorption dips due to the accretion stream implies $\beta < i$ and $\beta < 90°$, where i is the inclination and β the colatitude of the accretion spot.

Adopting the empirical period-mass and period-radius relations for Roche lobe filling secondaries from Patterson (1984), we obtain its mass to be 0.31 solar masses, and its radius to 0.36 solar radii, for masses of the white dwarf primary between 0.5 and 1.0 solar masses. This is in very good agreement with the spectroscopic classification of the secondary as an M4 dwarf, by Watson et al. (1994).

The 12150s modulation in optical light could be due to cyclotron beaming with maximum light when the magnetic field lines are at maximum angle to the line of sight. The double peak structure in the X-ray light curve can be interpreted as an absorption by the accretion funnel itself when the observer looks nearly parallel to the field lines above the accretion region (Inamura & Durisen 1983) and thus defines the meridian crossing of the accretion spot. This is supported by the fact, that the peaks seen in the optical light curves of Watson et al. (1994) occur prior to and after the double peak structure in the X-rays.

The low or absent soft X-ray flux in the phase interval outside the double peak is then caused by the occultation of the emission region by the white dwarf itself, when it disappears behind the limb as seen from the observer while the optical light emitted by the accretion funnel above the white dwarf surface is still visible.

Due to the asynchronous rotation the accretion geometry changes with phase of the beat period of 49.5d. Matter will couple onto different field lines and will thus be accreted in different positions relative to the axis of the magnetic field. Mukai (1988) showed, that the position of the accretion spot deviates substantially from that of the magnetic pole when the azimuth of the magnetical axis relative to the secondary is changed. In the case of QQ Vul, these longitudinal changes can amount to $-20°$ to +80° relative to the meridian defined by the direction to the secondary or $\pm 50°$ relative to the longitude of the magnetic pole.

We have measured the position of the double peak structure in the X-ray light curves by determining the centre of the eclipse like structure between them. The mean observation times of the three data sets from October 92, April 93 and October 93 are at beat period phases of 0.0, 0.17 and 0.18, if the first observation is taken as a reference. A linear fit results in a period of 12150.8s in good agreement with the optical data, but the residuals are very large, ranging from -490s to +280s. If they are attributed to longitudinal changes of the accretion spot on the white dwarf primary, they amount to $-15°$ to +8°. Thus they can be easily explained by the changing accretion geometry with beat phase.

Acknowledgements. We are grateful to the staff of the German-Spanish Astronomical Center for valuable suggestions and their assistance during the observing runs, and the Deutsche Forschungsgemeinschaft for financial support. We also thank the Director of the Mount Stromlo and Siding Spring Observatories for the opportunity to use the 2.3m telescope. We thank D. Campbell-Wilson for carrying out the radio observations at the Molonglo Synthesis Telescope. This work was supported in part by DARA grant 50 QR 90099

References

Beasley, A.J., Bastian, T.S., Ball, L., and Wu, K. 1994, AJ, 108, 2207
Beuermann, K., Schwope, A.D. 1993, Proc. 105th Meeting of the ASP, San Diego, July 1993
Beuermann, K., Burwitz, V. 1995, Proc. Cape Town Conf. on Magnetic CVs, Eds. B. Warner and D. Buckley, Jan. 1995, in press
Cropper, M. 1990, Space Science Reviews, 54, 195
Deeming, T.J. 1975, Ap&SS, 36, 137
Elvis, M., Lockman, F.J., Wilkes, B.J. 1989, AJ, 97, 777
Friedrich, S., Lamer, G., Staubert, R., and König, M. 1994, Astronomische Gesellschaft, Abstract Series No. 10, 149
Howell, S.B., Mitchell, K.J., WarnockIII A. 1988, AJ, 95, 247
Inamura, J.N.,Durisen, R.H. 1983, ApJ, 268, 291
Lamb, D.Q., Melia, F. 1987, Ap&SS, 131, 511
Leahy, D.A. 1983, ApJ, 272, 256
Madejski, G.M., Done, C., Turner, T.J., et al. 1993, Nat, 365, 626
Mittaz, J.P.D., Branduardi-Raymont, G. 1989, MNRAS, 238, 1029
Mukai, K. 1988, MNRAS, 232, 175
Newberry, M.V. 1991, PASP, 103, 122
Patterson, J. 1984, ApJS, 54, 443
Patterson, J. 1994, private communication
Rappaport, J., Verbunt, F., Joss, P.C. 1983, ApJ, 275, 713
Rosen, S., Done, C., Watson, M., Madejski, M.G. 1993, IAU Circ., No. 5850
Scargle, J.D. 1982, ApJ, 263, 835
Schwartz, U.J. 1978, A&A, 65, 345
Staubert, R., König, M., Friedrich, S., et al. 1994, A&A, 288, 513 (Paper I)
Staubert, R., Friedrich, S., Lamer, G., et al. 1995, Proc. Cape Town Conf. on Magnetic CVs, Eds. B. Warner and D. Buckley, Jan. 1995, in press
Stockman, H.S., Schmidt, G.D., Lamb, D.Q. 1988, ApJ, 332, 282
Verbunt, F., Zwaan, C. 1981, A&A, 100, L7
Watson, M.G., Rosen, S.R., O'Donoghue, D.et al. 1994, MNRAS, in press
Webbink, R.F. 1975, A&A, 41, 1
Weidemann, V., Koester, D. 1984, A&A, 132, 195

This article was processed by the author using Springer-Verlag LaTeX A&A style file *L-AA* version 3.